EXPERIMENTAL STUDY OF FREE-SURFACE AERATION AND TURBULENT PROCESSES DOWN AN EMBANKMENT DAM STEPPED SPILLWAY

González R. C. A.
Dept. of Civil Engineering, The University of Queensland, Brisbane QLD 4072, Australia.
Phone: +61 7 33653523, Fax: +61 7 33654599-E-mail:c.gonzalez@mailbox.uq.edu.au

Abstract: Research on stepped chute hydraulics has become an important tool for operational safety and design optimisation of these structures. Detailed experimental data is scarce and limited to very steep slopes ($\alpha>50^o$). This work details an experimental investigation of the physical flow characteristics of stepped chute flows conducted in a large-size laboratory model with a moderate slope typical of embankment dam slopes (h=0.1m, $\alpha=16^o$) operating with transition and skimming flow regimes. New original data include air concentration, air-water flow velocity and air-water flow turbulence intensity. The results suggest that air-water flow characteristics are not totally understood although there are some well-known features (eg. cavity recirculation) that influence significantly its behaviour in both skimming and transition flow conditions.

Keywords: stepped spillway, air entrainment, air-water flow properties, turbulence intensity, turbulent mixing layers, cavity re-circulation.

1. INTRODUCTION

Spillways are used to prevent dam overtopping caused by floodwaters. The design has changed through the centuries. In ancient times, some civilizations used steps to dissipate energy in open channels and dam overfalls in a similar fashion as in nature (eg. cascades) [4]. In the first half of the 20th century, the use of concrete became popular and the hydraulic jump-stilling basin was introduced as energy dissipator. The use of steps became obsolete and was replaced with smooth chutes followed by stilling basins. In recent years, new construction techniques and materials (RCC, PVC coated gabions, etc.) have allowed cheaper construction of stepped chutes. The development of new applications (eg re-aeration cascades and fish ladders) has increased the interest in stepped chute designs including their application for embankment dam overtopping [2],[4],[10]. Research on stepped chute flows prior to 1993 neglected the effect of free-surface aeration. Since, few studies focused on air-water flows in steep chutes but experimental data is still scarce. This paper details an experimental investigation of physical air-water flow characteristics down a stepped spillway conducted in a large-size laboratory model (h=0.1m) with a moderate slope ($\alpha=16^o$) typical of embankment dam slopes operating with transition and skimming flow regimes. A new analysis of air-water flow turbulence levels is presented providing original insights into air-water shear layers developing at each step edge in skimming flows.

2. EXPERIMENTAL APPARATUS AND INSTRUMENTATION

Experiments were conducted at the Hydraulics laboratory of the University of Queensland in a 3.75m long, 1m wide stepped chute (1V:3.5H slope, $\alpha=16^o$) operating with flow rates ranging from 0.046 to 0.219 m^3/s. The chute consisted of a broad crested weir with an upstream rounded corner followed by 9 identical steps (h=0.1m) and a horizontal stilling basin ending

into a pump sump. The pump was controlled with a Toshiba electronic transistor inverter ensuring a fine flow rate control during the experiments. The large size of the facility ensured minimum scale effects. Clear water depths were measured with point gauges while the flow rate was estimated from the measured head above crest with an accuracy of about 2%.
Air-water flow properties were measured using a double-tip conductivity probe developed at the University of Queensland that consisted of two tips (leading and trailing), aligned in the flow direction (Fig. 1). Each tip had an outer stainless steel electrode of 200µm and an inner platinum sensor of 25µm diameter. An air bubble detector (AS25240) excited the probe, translating the changes in conductivity into a voltage signal. A detailed description of the air bubble detector is reported in [2] and [8]. The probe signal was scanned at 20kHz for 20s per channel and processed using a program developed by [13]. Flow visualizations with a digital video camera (speed 25fr/s, shutter 1/4 to 1/6000s) were also conducted.
The probe displacement in the flow direction was conducted with a trolley system specifically designed for this purpose. The translation of the probe in the direction normal to the flow was controlled by a fine adjustment mechanism and measured with a Mitutoyo™ digital ruler. The accuracy on the transverse position of the probe was less than 0.2mm while the accuracy on the longitudinal position of the probe was estimated as $\Delta x = \pm 0.5$cm.

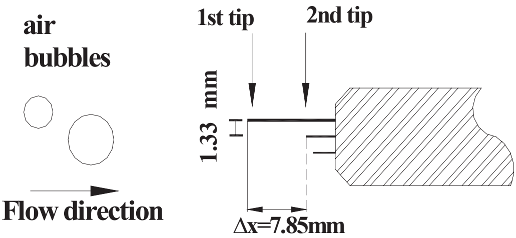

Figure 1 Double-tip conductivity probe (Top view).

3. EXPERIMENTAL MEASUREMENTS AND FLOW REGIMES.

Detailed experiments were performed for 14 water discharges ranging from 0.046 to 0.219m^3/s (Table 1). Measurements were conducted with the double-tip probe located at the channel centreline at each step edge and at several locations between edges (Fig. 2). In the direction normal to the flow, measurements were conducted from y=0 (i.e. pseudo-bottom formed by step edges) up to the spray region. In the flow direction measurements were recorded at step edges and at dimensionless distances X_0=0.25, 0.5 and 0.75 of L_{cav} where $X_0=x/L_{cav}$, x is the probe-tip distance to the upper step edge and L_{cav} is the distance between step edges ($L_{cav} = \sqrt{h^2 + l^2}$) (Fig. 2).

Table 1 Experimental flow conditions.

No	d_c/h	q_w (m^2/s)	Inception	Regime	Ref.
1	0.835	0.0756	3	Transition	RunQ76
2	0.06	0.0460	3	Transition	RunQ46
3	0.07	0.0580	3	Transition	RunQ58
4	0.09	0.0846	3	Transition	RunQ85
5	0.1	0.0990	4	Transition	RunQ99
6	0.11	0.1143	4	Transition	RunQ114
7	0.12	0.1302	between 4 and 5	Transition	RunQ130
8	0.13	0.1468	5	Transition/Skimming	RunQ147
9	0.14	0.1641	5	Skimming	RunQ164
10	0.15	0.1820	6	Skimming	RunQ182
11	0.16	0.2005	6	Skimming	RunQ200
12	0.17	0.2195	6	Skimming	RunQ219

At low flow rates, the flow cascaded down the stepped chute as a succession of free-falling nappes (nappe flow). Nappe flow was observed for small discharges $d_c/h<0.6$ where d_c is the critical flow depth and h the step height. (This flow was not investigated in this paper. Refer to [2],[4] and [13]). For large flow rates, the water skimmed over the pseudo-invert formed by the step edges (skimming flow). Skimming flow was observed for higher discharges $d_c/h>1.3$ (Fig. 3b). For a range of intermediate flow rates presence of air cavities between step edges, strong splashing and drop ejections were observed (transition flow) (Fig. 3a).

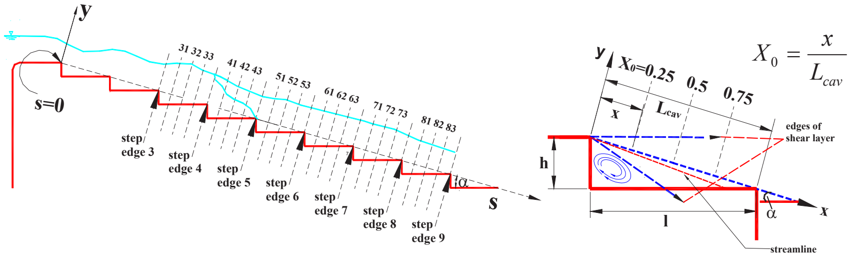

Figure 2 Measured locations.

In transition and skimming flows, the free surface was clear and transparent until the point of inception of air entrainment. At and downstream of this point, aeration took place and the flow became strongly turbulent (Fig. 3). The air-water flow layer extended throughout the fluid. In transition flow regime, the waters exhibited a chaotic behavior, strong spray near the free surface with drop ejections, intense free-surface aeration and different sized cavities between steps. For instance, a step cavity hosting a small air pocket was followed by a cavity partially filled with recirculating flow (Fig. 3a). In skimming flows, strong flow cavity recirculation was observed at all step cavities for all investigated flow rates. The vortices were best observed immediately next to the inception point with a small number of entrained air bubbles in the step cavity that enhanced visualization. Transfer of momentum and shear stress between mainstream and recirculating vortices maintained flow recirculation in the step cavities. At different time intervals, some recirculating cavity fluid flowed outwards to the mainstream and was replaced by new fluid. The ejection and inflow process took place typically near the downstream end of the cavity.

Chanson, Ohtsu and Yasuda [3], [5] hypothesized that in skimming flows, intense shear instabilities cause a separation at each step edge and a shear (mixing) layer develops with cavity recirculation underneath, whereas the mainstream loses momentum (Fig. 2).

a) b)

Figure 3 Transition and Skimming flow regime. a) Run Q76, $d_c/h=0.835, Q_w=0.076 m^3/s$. (Skimming Flow). b) Run Q147, $d_c/h=1.3$, $Q_w=0.147 m^3/s$ (Transition Flow).

4. AIR CONCENTRATION DISTRIBUTIONS

Dimensionless void fraction distributions measured downstream of the inception point of free-surface aeration for two discharges are presented in Figure 4. Results show rapid flow aeration in the downstream flow direction. Fig. 4a shows a skimming flow while Fig. 4b presents a transition flow. In skimming flows, experimental data measured at step edges and at the upstream end of the cavity ($X_0 \leq 0.25 L_{cav}$) compared favourably with an analytical solution of the air bubble advective diffusion equation:

$$C = 1 - \tanh^2\left(K - \frac{\frac{y}{Y_{90}}}{2D_0} + \frac{\left(\frac{y}{Y_{90}} - \frac{1}{3}\right)^3}{3D_0} \right) \tag{1}$$

where C is the void fraction, y is the distance measured normal to the pseudo bottom, Y_{90} is the characteristic distance (depth) where C reach 90%, K is an integration constant and D_0 is a function of the mean air concentration C_{mean} [5]:

$$C_{mean} = \frac{1}{Y_{90}} \int_0^{Y_{90}} C \, dy \tag{2}$$

Data obtained at the downstream end of cavities ($X_0/0.5L_{cav}$) suggested consistently a greater overall aeration of the flow than at step edges. This effect was particularly observed in the locations below the pseudo-bottom (i.e. y<0). It was proposed that inertial forces acting on air bubbles trapped in the centre of the recirculating vortices enhanced cavity aeration and lead to higher air content in the cavity flow and mixing layers that develop downstream of step corners [6],[9]. Void fraction distributions, observed in transition flows, indicated strong aeration throughout the entire flow cross-sections (Figure 4b). The data compared favourably with an analytical solution of the air bubble advective diffusion equation:

$$C = K'\left(1 - e^{\left(-\lambda \frac{y}{Y_{90}}\right)}\right) \tag{3}$$

where K' and λ are dimensionless coefficients function of C_{mean} [5].

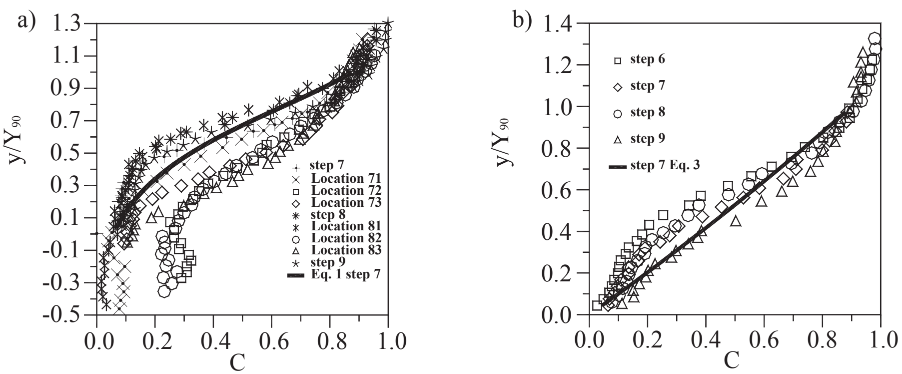

Figure 4 Void fraction profiles. (a) Run Q164 (Skimming). (b) Run Q85 (Transition).
(Data measured at the downstream end of the cavity ($X_0\langle 0.5$) is in white symbols).

5. AIR-WATER VELOCITY PROFILES.

Air-water flow velocity measurements were based upon the successive detection of bubbles by the two tips of the probe. In highly turbulent air-water flows, the detection of a bubble by each probe sensor is highly improbable, and it is common to use a cross-correlation technique [1],[7]. The time-averaged air-water velocity is defined as:

$$V = \frac{\Delta x}{T} \tag{4}$$

where Δx is the distance between probe sensors (Fig. 1) and T is the time travel for which the cross-correlation function is maximum [1],[6],[7]. Typical air-water velocity data are presented in Fig. 5. For skimming flows, the data collected at step edges compared reasonably with a power law.

$$\frac{V}{V_{90}} = \left(\frac{y}{Y_{90}}\right)^{\frac{1}{N}}, \qquad \frac{y}{Y_{90}} \leq 1 \tag{5}$$

where V_{90} is the characteristic velocity at $Y=Y_{90}$ (Fig. 5a) and $7.8<N<11.8$ for $1.3<d_c/h<1.7$. Between step edges, skimming flows velocity profiles did not follow Eq. 5 (Refer to the following paragraph for further discussion). Transition flow velocity profiles suggested that air water velocity distributions at step edges are nearly uniform, as observed down a 22^o slope chute by [5].

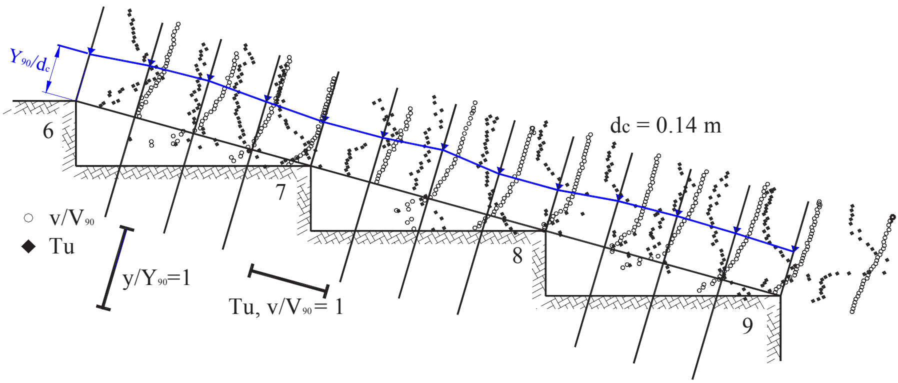

Figure 5 Air-water velocity and turbulence intensity profiles in skimming flow (Run Q164). (White symbols: velocity. Black symbols: Turbulence intensity).

DISCUSSION

A series of detailed measurements were conducted between step edges at the last cavity of the chute for one discharge ($d_c/h=1.7$) to gain a better understanding of momentum exchange between mainstream and flow re-circulation. The data were compared successfully with analytical solutions of the motion equation for plane turbulent shear layers developed by Tollmien and Goertler [11],[12].

Results are presented in figures 6 and 7 where u/U_0 is the dimensionless velocity; U_0 is a measure of the free-stream velocity taken as $U_0=0.9V_{90}$, $\xi=\sigma y/x$ and σ is an empirical constant, experimental values ($2.5<\sigma<6$) showed a tendency towards the reported value for monophase flow ($\sigma=11$) in [11].

The findings indicate that the velocity profiles agree well with Tollmien's and Goertler's solutions and demonstrate self-similarity in the developing mixing layer (Fig. 6).
Experimental observations of the developing shear layer upper edge (i.e. depth where $u/U_0=1$) and of the streamline $u/U_0=0.5$ (i.e. depth y_{50}) are reported in Fig. 7. The data follow a trend somehow similar to free mixing layer in monophase flow although the apparent width of mixing layer does not increase linearly with x as hypothesized by Goertler.
The finding strongly supports the hypothesis that a shear layer develops at each step edge, plays a major role in the air-water flow behaviour inside the recirculation cavities, and affects the overall flow resistance, providing means to predict the growth rate of the mixing layer and to calculate the mean velocity distribution and the turbulence shear stress.

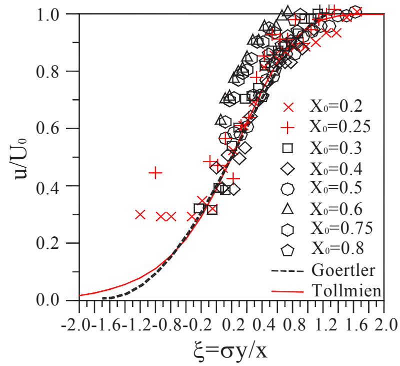

Figure 6 Experimental data compared with Tollmien and Goertler solution.

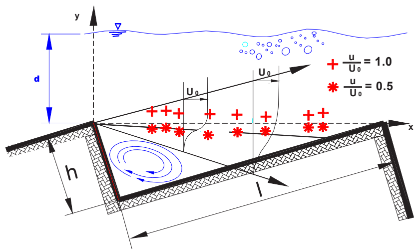

Figure 7 Sketch of the developing shear layer compared with experimental data.

6. TURBULENCE INTENSITY

Turbulence intensity $Tu=u'/V$ is a dimensionless measure of the turbulent fluctuations of interfacial velocity over the distance separating the probe sensors [6], [7].
Its measure is related to the broadening of the cross-correlation function compared to the auto-correlation function [5],[6]:

$$Tu = \frac{u'}{V} = 0.851\frac{\sqrt{\Delta T^2 - \Delta t^2}}{T} \qquad (6)$$

where u' is the root mean square of the longitudinal component of turbulent velocity, V is the local time-averaged air-water velocity, ΔT is the time scale satisfying $r(T+\Delta T)=R_{max}/2$, r is the cross-correlation coefficient function and R_{max} is the maximum cross-correlation, Δt is the characteristic time for which the autocorrelation function equals 0.5, and T is the time travel for which the cross-correlation function is maximum. Eq.6 is based upon an extension of the mean value theorem for definite integrals [5],[6].
Air-water flow turbulence intensity (Tu) profiles are presented in Fig. 5 (black symbols). The data show very high turbulence levels. Despite of the high turbulence levels measurements at the upstream end of the cavity followed a trend similar in shape to LDA turbulence intensity measurements in monophase flows [10], and in monophase free-shear layers [14], while profiles collected at the downstream end of the cavity exhibited a significantly different shape (i.e. suggesting higher turbulence intensity levels at locations below the pseudo-bottom).

DISCUSSION

It is believed that high rate of energy dissipation, associated with form drag generated by the steps, contributes to strong turbulent mixing throughout the entire flow, which yields high turbulence intensity levels. Chanson and Toombes [6] hypothesized that the increase in turbulence level is directly linked to the number of entrained bubbles/droplets. Further comparisons between turbulence intensity data and bubble count rate reflected this behavior. However, increase in turbulent velocity may be also attributed to other factors, including particle collisions, breakup and coalescence, which affect the interfacial velocity field [6].

7. CONCLUSION

New experiments were conducted in a large-size stepped channel corresponding to an embankment-overtopping chute. Turbulent air-water flow properties were measured with a double-tip conductivity probe. The results show intense shear instabilities caused by separation at each step edge while a shear layer develops downstream of each step edge associated with momentum transfer between the main flow and recirculation cavities.

Void fraction data in skimming flows showed dtrong flow aeration at the upstream end of the cavities in the downstream flow direction and compared favourably with an analytical solution of air bubble diffusion equation. Measurements at the downstream end of step cavities suggested greater overall flow aeration than those at the upstream end, particularly at locations below the pseudo-bottom. This finding supports the suggestion that inertial forces act on air bubbles trapped in the core of the recirculating vortices enhancing aeration in the cavity. Void fraction measurements in transition flows indicated strong aeration throughout the entire flow cross-sections and compared favourably with another solution of the air bubble advective diffusion equation.

Between step edges, experimental velocity profiles agreed well with Tollmien's and Goertler‘s solutions of the motion equation for plane turbulent shear layers and demonstrated self-similarity in the developing mixing layer. The result provides means to predict the growth of the mixing layer and to calculate the mean velocity distribution and turbulence shear stress.

Turbulence intensity (Tu) profiles showed very high turbulence levels. Measurements at the upstream end of cavities followed a trend similar to previously observed LDA turbulence intensity measurements in monophase flows [10],[14], while profiles collected at the downstream end of the cavity exhibited a different shape suggesting higher turbulence levels at locations below the pseudo-bottom.

ACKNOWLEDGEMENTS

The writer thanks Dr. H. Chanson and Dr. John Macintosh for helpful reviews; Dr. L. Toombes and Mr. D. Callaghan and Mr. Graham Illidge for their assistance and The National Council for Science and Technology of Mexico (CONACYT) for its financial support.

REFERENCES

1. Chanson, H. (1997b). "Air Bubble Entrainment in Free-Surface Turbulent Shear Flows." *Academic Press*, London, UK, 401 pages.
2. Chanson, H. (1998). "Review of studies on Stepped Channel flows." *Workshop on Flow Characteristics around hydraulic structures and River Environment*. University Research Center, Nihon University, Japan.
3. Chanson, H., Yasuda Y., and Ohtsu I. (2000). "Flow resistance in Skimming Flow: A Critical Review." *Intl. Workshop on Hydraulics of stepped spillways, H.E Minor & W.H. Hager Balkema Publishers,* Zurich, Switzerland.

4. Chanson, H. (2002). “The Hydraulics of Stepped Chutes and Spillways.” *Balkema Publishers*, Rotterdam, The Netherlands.
5. Chanson, H., and Toombes, L. (2002). “Experimental Investigations of Air Entrainment in Transition and skimming flows down a stepped chute” *Can. Jl. Civ. Eng*, Vol.29, pp. 145-156 pages.
6. Chanson, H., and Toombes, L. (2002). “Air-Water Flows down Stepped chutes: Turbulence and Flow Structure Observations.” *Intl Jl of Multiphase Flow*, Vol. 27, No.11, pp. 1737-1761.
7. Crowe, C., Sommerfeld, M., and TSUJI, Y. (1998). “Multiphase Flows with Droplets and Particles.” *CRC Press*, Boca Raton, USA, 471 pages.
8. Cummings, P.D. (1996). “Aeration due to breaking waves.” Ph.D Thesis, *The University of Queensland*, Brisbane, Australia.
9. Matos, J., Yasuda, Y., and Chanson, H. (2001). “Interaction between free-surface aeration and cavity re-circulation in skimming flows down stepped chutes.” *Proc. XXIX IAHR Congress,* Beijing, China, Theme D, pp. 611-617.
10. Ohtsu, I., and Yasuda, Y. (1997). “Characteristics of Flow Conditions on Stepped Channels.” *Proc. XXVII IAHR Congress*, San Francisco, USA, Theme D, pp. 583-588.
11. Rajaratnam, N. (1976). “Turbulent jet flows.” *Elsevier,* Amsterdam, The Netherlands.
12. Schlichting, H. (1979). “Boundary Layer Theory.” *McGraw-Hill*, New York, USA, 7th edition.
13. Toombes, L. (2002). “Experimental Study of Air-water flow properties on low-gradient stepped cascades.” Ph.D. Thesis, *The University of Queensland*, Brisbane, Australia.
14. Wygnansky, I. and Fiedler, H. (1970). “The Two-dimensional Mixing Region.” *Jl. Of Fluid mechanics*, Vol.41, pp. 327-361.